

See discussions, stats, and author profiles for this publication at: <https://www.researchgate.net/publication/256765508>

Hybrid Nanospheres Formed by Intermixed Double-Hydrophilic Block Copolymer Poly(ethylene oxide)-block-poly(2-ethyloxazoline) with High Content of Metallacarboranes

ARTICLE *in* MACROMOLECULES · AUGUST 2013

Impact Factor: 5.8 · DOI: 10.1021/ma4013626

CITATIONS

5

READS

58

8 AUTHORS, INCLUDING:



[Mariusz Uchman](#)

Charles University in Prague

35 PUBLICATIONS 326 CITATIONS

[SEE PROFILE](#)



[Antti Nykänen](#)

National Institute of Metrology, Quality and Te...

45 PUBLICATIONS 1,522 CITATIONS

[SEE PROFILE](#)



[Janne Ruokolainen](#)

Aalto University

216 PUBLICATIONS 6,582 CITATIONS

[SEE PROFILE](#)



[Pavel Matejicek](#)

Charles University in Prague

46 PUBLICATIONS 516 CITATIONS

[SEE PROFILE](#)

Hybrid Nanospheres Formed by Intermixed Double-Hydrophilic Block Copolymer Poly(ethylene oxide)-block-poly(2-ethyloxazoline) with High Content of Metallacarboranes

Vladimír Ďordovič,[†] Mariusz Uchman,[†] Karel Procházka,[†] Alexander Zhigunov,[‡] Josef Pleštil,[‡] Antti Nykänen,[§] Janne Ruokolainen,[§] and Pavel Matějíček^{*,†}

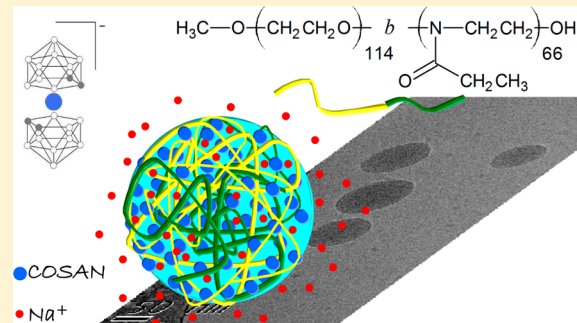
[†]Department of Physical and Macromolecular Chemistry, Faculty of Science, Charles University, Hlavova 2030, 128 40 Prague 2, Czech Republic

[‡]Institute of Macromolecular Chemistry, v.v.i., Academy of Sciences of the Czech Republic, Heyrovský Sq. 2, 16206 Prague 6, Czech Republic

[§]Department of Applied Physics Nanotalo, Aalto University, Puumiehenkuja 2, FI-02150 Espoo, Finland

Supporting Information

ABSTRACT: In search for biocompatible hydrophilic polymers suitable for preparation of delivery systems of boron cluster compounds with high loading capacity, we studied the interaction of metallacarborane sodium [3-cobalt(III) bis(1,2-dicarbollide)] with poly(2-ethyloxazoline) (PEOX) and with a double-hydrophilic block copolymer poly(ethylene oxide)-block-poly(2-ethyloxazoline) (PEO–PEOX) in aqueous solutions by a combination of scattering, microscopy, spectroscopy, and thermochemistry techniques. The paper is a contribution to our long-time study of novel hybrid nanostructures based on hydrophilic polymer–metallacarborane complexes. PEOX homopolymer interacts with metallacarborane, resulting in a water-soluble, negatively charged complex. In the case of diblock copolymer PEO–PEOX, both blocks interact with metallacarborane via dihydrogen bonds and participate in the formation of hybrid gel-like nanostructures in 0.1 M NaCl aqueous solutions, which are unique as compared to other boron cluster-containing polymeric systems. The stable spherical nanoparticles with high metallacarborane content do not adopt core/shell structure, which has been observed for other PEO-containing double hydrophilic block copolymers [*Macromolecules* 2009, 42, 4829], but the nanospheres are homogeneous. They contain intermixed PEO and PEOX blocks, which are cross-linked by metallacarborane molecules. The size of the nanospheres depends on a preparation protocol, while their inner structure does not. Besides the detailed study on PEO–PEOX/metallacarborane system, a high application potential of PEO–PEOX complexes with several metallacarborane-based drugs is also shown. The study clearly demonstrates that PEOX is suitable polymer for designing novel hybrid nanostructures.



INTRODUCTION

Metallacarboranes belong to promising species in medicine,^{1a–s} and they find applications also in other fields.^{2a–f} Some years ago we started a systematic research on the solution behavior of [3-cobalt(III) bis(1,2-dicarbollide)][–] anion, **1**, and the interaction of related metallacarboranes with polymers, surfactants, and cyclodextrins in aqueous solutions.^{3a–e} Our interest was promoted by the discovery of a strong inhibition activity of several metallacarborane conjugates toward HIV protease.^{4a–d} However, the use of boron cluster-based inhibitors is complicated by their complex behavior in aqueous solutions. They are almost always sparingly soluble and form peculiar aggregates in water, which represents a problematic point in the research and applications.^{4d,e} The key challenge is to prepare well-defined, biocompatible, and stable dispersions of boron cluster compounds in water which could be directly applied in drug delivery.^{5a–f} Hence, the task we are dealing with

is how to stabilize metallacarboranes in aqueous media, and it is not directly targeted at the increase of inhibition activity.

Recently, we published a couple of papers on the interaction of **1** with high-molar-mass poly(ethylene oxide), PEO.^{6a–c} The PEO/**1** complex is not soluble in water, but its formation can be controlled and tuned by a salt concentration.^{6a} As revealed by WAXS and solid-state NMR study, the PEO/**1** nanocomposite has an interesting inner structure—the metallacarborane clusters and sodium counterions are uniquely organized within the amorphous PEO matrix.^{6b} The fact that the PEO/**1** complex does not dissolve in water precludes the use of PEO (PEG) as a stabilizing block in polymeric nanostructures for the delivery of metallacarboranes. Never-

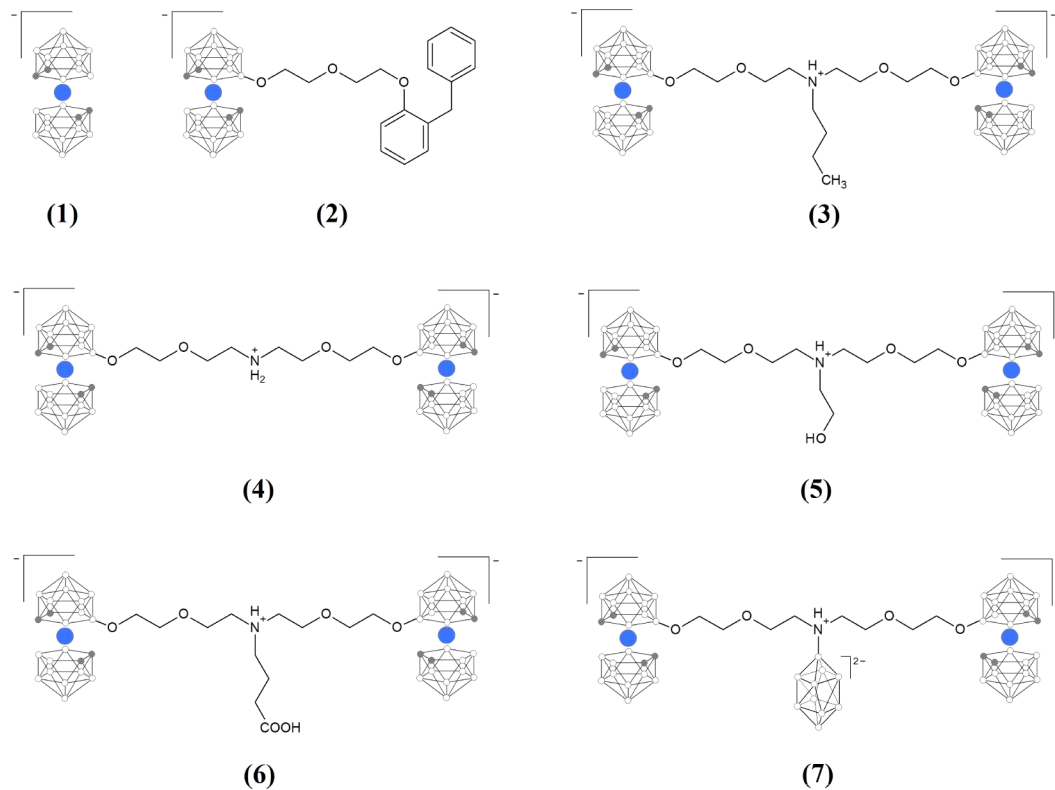
Received: June 30, 2013

Revised: August 5, 2013

Published: August 22, 2013



Scheme 1. Structures of All Metallacarboranes Used in Our Study



theless, this disadvantage can be turned into an advantage: In our recent papers, we proposed a scenario where the PEO block of poly(methacrylic acid)-block-poly(ethylene oxide) diblock copolymer, PMA–PEO, was used as the “carrier” of metallacarboranes. It is the first example in the literature where the PEO block is present in the core of core/shell nanoparticles, which are stabilized by charged PMA blocks in alkaline buffers.^{6a,c} Even though the PMA–PEO/1 micelles are very stable and stimuli-responsive in aqueous solutions, the PMA block is not biocompatible, and hence the entire system is not suitable for drug-delivery applications.^{6c} Therefore, we continue in screening of other potentially applicable polymers, which however retain PEO block in their structure as a part capable to bind boron cluster compounds. In the simplest possible case, we would like to replace the PMA block by a more suitable one.

In this work, we address the question of the use of poly(alkyloxazolines), POX, as stabilizing blocks of metallacarborane containing hybrid nanoparticles. The interest in POX as a polymer component of various therapeutics has been rapidly increasing as it can be documented by the relevant literature.^{7a,b} Here, we study in detail basic principles that control the interaction of parent sodium cobalt bis(dicarbollide), 1, with linear homopolymer poly(2-ethyloxazoline), PEOX, and that influence the size and the morphology of nanoparticles formed by double-hydrophilic block copolymer PEO–PEOX and 1 in aqueous solutions. We have chosen PEO–PEOX copolymer because it is fully biocompatible. The individual blocks (PEO and PEOX) are assumed to have following functions: PEO should bind metallacarborane molecules in the form of insoluble complex, while PEOX should keep the nanoparticle dispersed in solution. Further, as the PEO/1 complex is sensitive to the cation concentration,^{6a}

we expected that the system could be stimuli-responsive with respect to a salt concentration. The nanoparticles were characterized by standard scattering (SLS&DLS and SAXS), microscopy (AFM and cryo-TEM), spectroscopy (NMR and UV-vis), and thermochemistry (ITC) techniques. In order to justify the importance of the present study, we included a brief survey of selected data on the interaction of PEO–PEOX with metallacarborane conjugates, 2–7, which are efficient inhibitors of HIV protease (structures shown in Scheme 1). A detailed study of those conjugates is in progress, and more detailed information will be presented soon in a medicine-oriented journal. In our future research, we are also planning to pay attention to the role of counterions in self-assembling processes of metallacarboranes. However, in the present communication as well as in all our previous projects we work exclusively with sodium salts.

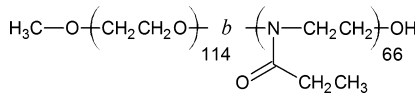
EXPERIMENTAL SECTION

Materials. Metallacarborane sodium [3-cobalt bis(1,2-dicarbollide)]⁻, Na[1], was a kind gift of Bohumír Grünér and Jaromír Plešek (Institute of Inorganic Chemistry, Academy of Science of the Czech Republic, Řež, near Prague). It has been characterized using mass spectrometry and ¹H and ¹¹B NMR spectroscopy and in aqueous solutions by other techniques.^{3a} Metallacarborane conjugates GB42 (2), GB48 (3), GB80 (4), GB105 (5), GB124 (6), and GB225 (7) were prepared in a form of sodium salts by Bohumír Grünér and designed as HIV protease inhibitors.^{4a–e} Structures of all metallacarborane samples are shown in Scheme 1.

The poly(ethylene oxide)-block-poly(2-ethyl oxazoline), PEO–PEOX, block copolymer was purchased from Polymer Source, Inc. (Dorval, Quebec, Canada). The weight-averaged relative molecular weight of the PEO and the PEOX block, provided by the manufacturer, are 5.0×10^3 and 6.5×10^3 , respectively, with dispersity 1.4. The poly(2-ethyloxazoline) linear polymer was purchased from

Aldrich with the weight-averaged relative molecular weight 5×10^4 . The structure of PEO–PEOX is shown in Scheme 2.

Scheme 2. Structures of Double-Hydrophilic Block Copolymer Poly(ethylene oxide)-block-poly(2-ethyloxazoline) (PEO–PEOX) As Provided by the Manufacturer



Sample Preparation. The light scattering (LS) titration experiments for monitoring of the nanoparticle formation were carried out as follows: Stock aqueous solution of Na[1] (0.0245 M) was consecutively added to PEO–PEOX solutions (2 g/L, 5 mL) in water, 0.01 M NaCl, and 0.1 M NaCl. A time lag between each addition was around 2 h. Since the nanoparticles, which form during the LS titration, are strong scatterers, we performed the LS study with relatively diluted solutions. The solutions during the titration process were analyzed by a measuring of light scattering, AFM, and cryoTEM.

The samples for SAXS study were prepared by quick addition of Na[1] solution in 0.1 M NaCl to 200 μL of relatively concentrated PEO–PEOX solution (10 g/L) in 0.1 M NaCl.

The samples for NMR study were prepared by mixing of calculated amount of solid Na[1] with 2 mL of PEO–PEOX solution (10 g/L) in 0.00, 0.01, and 0.10 M NaCl in D_2O in order to obtain mixtures with 1-to-polymer segment ratio $\xi = 0.015$ and 0.045. A small amount of *tert*-butyl alcohol (*t*-BuOH) was added to the solutions as an internal standard. We used polymer solutions with relatively high concentration of polymer for NMR to get signals of sufficient quality. As a smaller amount of solution is needed for NMR as compared to LS titration, we directly added the appropriate amount of solid sample to the polymer solution to skip the unstable region (low content of metallacarborane).

In experiments with HIV protease inhibitors, 3 mg of GB42 (2), GB48 (3), GB80 (4), GB105 (5), GB124 (6), and GB225 (7) were mixed with 2 mL of water, physiological saline (154 M NaCl) with/without copolymer PEO–PEOX (10 g/L). All the mixtures were sonicated (30 min) and left to shake overnight. The metallacarborane content was obtained by measuring of UV-vis of clear centrifugated solutions.

We did investigate whether the mixing protocol affects the structure of obtained nanoassemblies. We studied the nanostructures prepared from polymer solutions of different concentration by various scattering techniques. We observed that the well-behaving nanospheres are formed both by slow mixing of dilute solutions and by fast mixing of concentrated solutions. An important fact is that the excess of metallacarborane stabilizes the nanoparticles in solution. Since the nanospheres are homogeneous, their inner structure is not affected by the preparation protocol as proven by SAXS and NMR. Different mixing procedures result in different dimensions of the nanoparticles only: the slower titration rate provides larger and less stable nanoparticles. All samples for NMR, SAXS, and other studies were also characterized by LS measurements.

Methods. *Dynamic Light Scattering (DLS) and Static Light Scattering (SLS).* The light scattering setup (ALV, Langen, Germany) consisted of a 633 nm He–Ne laser, an ALV CGS/8F goniometer, an ALV High QE APD detector, and an ALV 5000/EPP multibit, multiautocorrelator. DLS data analysis was performed by fitting the measured normalized intensity autocorrelation function $g_2(t) = 1 + \beta|g_1(t)|^2$, where $g_1(t)$ is the electric field correlation function, t is the lag time, and β is a factor accounting for deviation from the ideal correlation. An inverse Laplace transform of $g_1(t)$ with the aid of a constrained regularization algorithm (CONTIN) provides the distribution of relaxation times, $\tau_A(\tau)$. Effective angle- and concentration-dependent hydrodynamic radii, $R_H(q,c)$, were obtained from the mean values of relaxation times, $\tau_m(q,c)$, of individual diffusive modes using the Stokes–Einstein equation. To obtain true

hydrodynamic radii, the data have to be extrapolated to a zero scattering angle. Since the refractive index increment, dn/dc , is unknown for almost all of the samples, we evaluated in such cases only the light scattering intensity extrapolated to zero scattering angle as the measure proportional to molar mass of polymeric nanoparticles. The SLS data for the sample PEO–PEOX/1 in 0.1 M NaCl with 1-to-polymer segment ratio $\xi = 0.153$ were treated by the standard Zimm method with $dn/dc = 0.196 \text{ mL/g}$ measured with the Optilab T-rEX refractive index detector, Wyatt Technology Corporation.

Electrophoretic Light Scattering. The measurements were carried out with a Nano-ZS Zetasizer (Malvern Instruments, UK). Zeta-potential values were calculated from electrophoretic mobilities (averages of 15–100 measurements) using the Smoluchowski approximation.

UV-vis Spectroscopy. UV-vis absorption spectra were carried out with a Hewlett-Packard 8452a diode-array spectrometer.

Atomic Force Microscopy (AFM). AFM measurements were performed in the semicontact (tapping) mode under ambient conditions using a scanning probe microscope Digital Instruments NanoScope dimensions 3 equipped with a Nanosensors silicon cantilever. The nanoparticles were deposited from very dilute solutions (ca. 0.01 g/L) on a freshly cleaved mica surface. The samples were left to dry in a vacuum oven.

Cryo-Transmission Electron Microscopy (Cryo-TEM). Cryo-TEM was carried out using field emission cryo-electron microscope (JEOL JEM-3200FSC), which was operating at 300 kV voltage. Images were taken in bright field mode and using zero loss energy filtering (omega type) with the slit width of 20 eV. Micrographs were recorded using Gatan Ultrascan 4000 CCD camera. Specimen temperature was maintained at -187°C during the imaging. Vitrified specimens were prepared using automated FEI Vitrobot device using Quantifoil 3.5/1 holey carbon copper grids with the hole size of 3.5 μm . Just prior to use grids were plasma cleaned by Gatan Solarus 9500 plasma cleaner and then transferred into an environmental chamber of FEI Vitrobot having room temperature and 100% humidity. Thereafter 3 μL of sample solution was applied on the grid, and it was blotted once for 1 s and then vitrified in 1/1 mixture of liquid ethane and propane at temperature of -180°C . The grid with vitrified sample solution was maintained at liquid nitrogen temperature and then cryo-transferred into the microscope.

Small Angle X-ray Scattering (SAXS). SAXS experiments were performed using a pinhole camera (Molecular Metrology SAXS System) attached to a microfocused X-ray beam generator (Osmic MicroMax 002) operating at 45 kV and 0.66 mA (30 W). The camera was equipped with a multiwire gas-filled area detector with an active area diameter of 20 cm (Gabriel Design). Two experimental setups were used to cover the q range of $0.005\text{--}1.1 \text{ \AA}^{-1}$. The scattering vector, q , is defined as $q = (4\pi/\lambda) \sin \theta/2$, where λ is the wavelength and 2θ is the scattering angle. The scattering intensities were put on absolute scale using a glassy carbon standard.

¹H NMR Spectroscopy. ¹H NMR spectra were measured on a Varian UNITYINOVA 400 in deuterium oxide (99.5%; Chemotrade, Leipzig, Germany). Spectra were referenced to the solvent signal (4.80 ppm).

Isothermal Titration Calorimetry (ITC). ITC measurements were performed with an isothermal titration calorimeter (Nano ITC), TA Instruments - Waters LLC, New Castle, DE. The microcalorimeter consists of a reference cell and a sample cell (24K gold). The sample cell is connected to a 100 (50) μL syringe. The syringe needle is equipped with a flattened, twisted paddle at the tip, which ensures continuous mixing of the solutions in the cell rotating at 200 (250) rpm. Titrations were carried out by consecutive 5 μL injections of 24.5 mM NaCoD (1) in 0.00, 0.01, and 0.10 M NaCl aqueous solutions from the syringe into the sample cell filled with 960 (193) μL of 0.5 g/L PEO–PEOX and PEOX in 0.00, 0.01, and 0.10 M NaCl aqueous solution. A total of 20 injections were performed with intervals of 1800 s. These injections replace a part of the solution in the sample volume, and the changed concentration is considered in the calculation of the sample concentration. By this method then the differential heat of mixing is determined for discrete changes of composition. The data

were analyzed using the NanoAnalyze software by fitting with a simple one-site binding model.

RESULTS AND DISCUSSION

Our preliminary study of aqueous mixtures containing metallacarborane **Na[1]** (see Scheme 1) and homopolymer poly(2-ethyloxazoline), PEOX, has shown that the components interact with each other. Even though PEOX and **1** form the complex, a copolymer with PEOX blocks can be still useful for our purposes because PEOX/**1** is soluble in water and NaCl solutions (details discussed below). In order to quantify the affinity of metallacarborane to PEOX homopolymer and to diblock copolymer PEO–PEOX (see Scheme 2), we carried out a set of dialysis experiments according to our previous papers.^{6a} The number of polymer segments interacting with one metallacarborane cluster was estimated by means of UV-vis absorption of **1** in a dialysis bath when monitoring the concentration change (uptake) of **1** by PEOX and PEO–PEOX, which were placed in the semipermeable dialysis tube. We performed the studies in pure water and in NaCl solutions up to 0.1 M because we found earlier that the presence of salt affects strongly the interaction of cobalt bis(dicarbollides) with hydrophilic polymers.^{6a} The following values have been obtained for PEOX and PEO–PEOX with different salt concentrations (0.00, 0.01, and 0.10 M NaCl): PEOX (9; 9; 9) and PEO–PEOX (19; 18; 6), respectively. The values for PEO have been already reported^{6a} and are as follows: PEO (500; 18; 10), respectively. It is evident that the affinity of PEOX homopolymer as well as PEO–PEOX block copolymer to metallacarborane is significant. Further, it is only slightly dependent on NaCl concentration, which is not definitely true for PEO homopolymer.

During the dialysis study, we noticed that PEOX/**1** complex, which formed within the dialysis tube, does not precipitate as it was observed in the case of PEO/**1** in NaCl solutions. Even light scattering measurements of PEOX/**1** did not detect a presence of large aggregates, which would have been accompanied by a significant increase of light scattering intensity and eventually would have led to a quantitative precipitation. The mixtures predominantly consist of free PEOX chains probably decorated by **1** clusters, **Na[1]** self-assemblies,^{3a} and a low fraction of multimolecular PEOX/**1** aggregates, the dimension of which adopts the size of metallacarborane aggregates.^{6c} Since ¹H NMR spectra (not shown) of PEOX involved in the complex are relatively broad indicating a hindrance of segmental motion in PEOX/**1**, we assume that a specific interaction between PEOX and **1** does play a role.

To get a deeper insight into the structure of the PEOX/**1** complex, we compare it with a reasonable “reference system”—the PEO/**1** nanocomposite—the structure of which has been described in detail by quantum chemistry, WAXS, and solid state NMR.^{6c} We similarly assume that the ethylene subunits of PEOX backbone interact with hydrogen atoms of boron clusters of **1** via dihydrogen bonds. Previous studies have also shown that not only the dihydrogen bonds but also the interaction of sodium counterion with PEO plays a significant role in the complex stabilization. Since Na⁺ ions do not interact with amidic groups in the PEOX segments,⁸ one of the crucial conditions for the complex precipitation is not fulfilled in this case, and PEOX/**1** is therefore soluble in aqueous media.

Knowing the above-mentioned details on PEOX/metallacarborane interaction, we performed a systematic study on the

coassembly of **1** with diblock copolymer PEO–PEOX with the aim to prepare stable nanoparticles with the highest possible loading capacity in NaCl aqueous solutions (close to physiological conditions). In analogy with our previous studies on the interaction of **1** with PEO,^{6a,c} we prepared the hybrid nanoparticles by a titration of PEO–PEOX dilute solutions by **Na[1]** as described in the Experimental Section. The formation of nanoparticles at different steps of the titration was monitored by several experimental techniques (scattering, spectroscopy, and microscopy). Results of individual techniques will be presented and discussed below. We also explored the role of the mixing protocol (PEO–PEOX with **1**) as described in one paragraph of the Experimental Section.

Basic Characterization of the Self-Assembly by Light Scattering

At first, we performed the light scattering study. We monitored the formation of aggregates by static and dynamic light scattering (SLS&DLS) during the titration of PEO–PEOX (*c* = 2 g/L) by **Na[1]**. Dependencies of SLS intensity and hydrodynamic radius (R_H), both extrapolated to the zero scattering angle, on 1-to-polymer segment ratio, ξ (the sum of PEO and PEOX segments is taken into account), are shown in Figures 1 and 2, respectively. Since PEO–PEOX is a

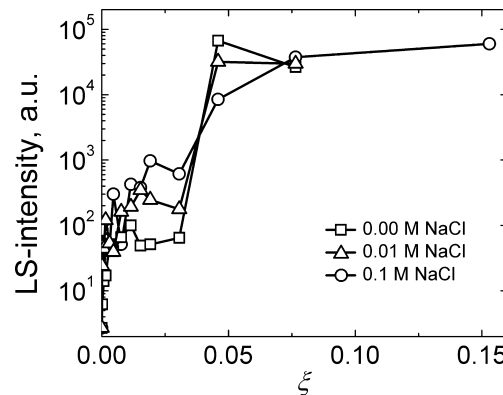


Figure 1. Dependence of light scattering intensity on the addition of **Na[1]** to PEO–PEOX solution (2 g/L) in (squares) 0.00 M, (triangles) 0.01 M, and (circles) 0.10 M NaCl.

double-hydrophilic block copolymer, the SLS intensity of the pure copolymer solution is very weak, and the principal diffusion mode measured by DLS corresponds to the size of

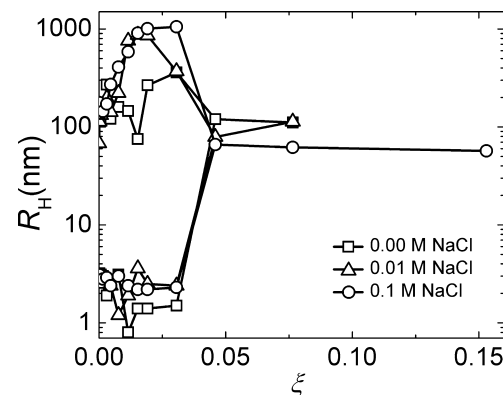


Figure 2. Dependence of hydrodynamic radius, R_H , on the addition of **Na[1]** to PEO–PEOX solution (2 g/L) in (squares) 0.00 M, (triangles) 0.01 M, and (circles) 0.10 M NaCl.

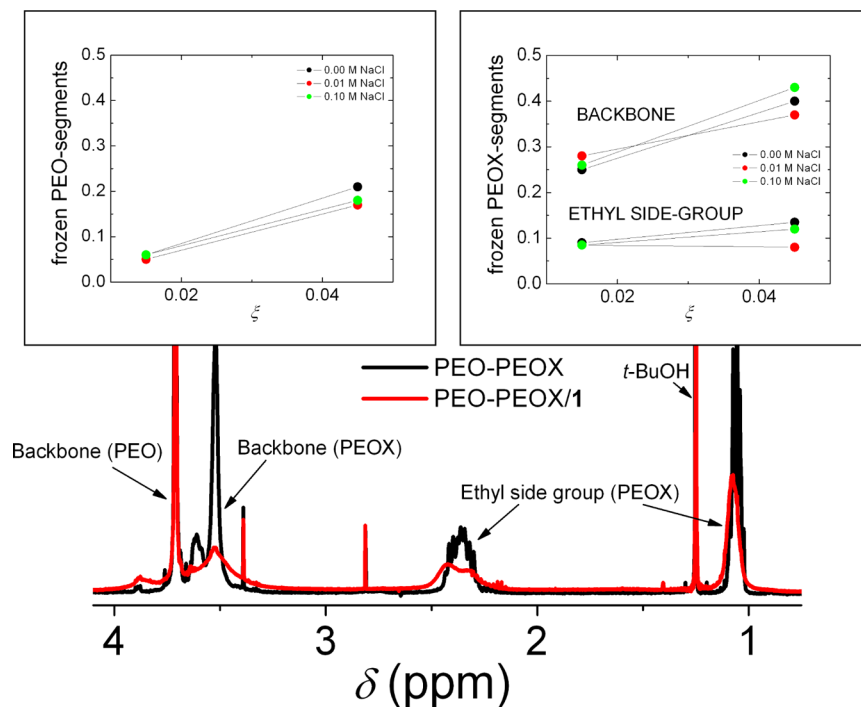


Figure 3. Typical ^1H NMR spectra of (black line) PEO–PEOX and (red line) PEO–PEOX/1 ($\xi = 0.045$; 0.1 M NaCl) with *t*-butanol as an internal standard. Inset: fraction of frozen segments of PEO (left) and PEOX (right) in PEO–PEOX/1 differing in Na[1] content and NaCl concentration calculated from a decrease of corresponding ^1H NMR signals related to pure PEO–PEOX and *t*-butanol.

polymer coils (R_{H} ca. 3 nm). We detected also a small amount of large aggregates as described recently in the literature.⁹ The addition of **1** leads to a steep increase of the scattering intensity. As seen in Figures 1 and 2, we can distinguish two aggregation regions depending on ξ . In the first one (for $\xi < 0.05$), the scattering intensity increases ca. 10^2 times. The DLS distribution of relaxation times is bimodal in this region (shown in Figure S1 of the Supporting Information). Small scatterers with dimensions of few nanometers (most probably the single PEO–PEOX chains) coexist with polydisperse and long-time unstable aggregates appreciably larger than 100 nm. A relatively low scattering intensity in this region suggests that the large aggregates are not compact particles and that their concentration is low which can be deduced also from the distributions of relaxation times if we take into account that the scattering power is proportional to R_{H}^6 (see Figure S1).

The scattering intensity rises steeply in the second region ($\xi > 0.05$), and it remains almost constant in 0.1 M NaCl (other solutions are unstable in this region). It is worth mentioning that the Zimm plot measured for the nanoparticles with $\xi = 0.153$ in 0.1 M NaCl is regular (see Figure S2). From the Zimm plot, we evaluated the mass-average molar mass of the PEO–PEOX/1 nanoparticles (in 0.10 M NaCl; $\xi = 0.153$) and obtained the following value: $M_w = 231 \times 10^6$ g/mol (PEO–PEOX aggregation number N^{agg} ca. 11 000; $w(\text{Na}[1]) = 55.5\%$). Their hydrodynamic radius obtained from the dynamic Zimm plot is 69 nm. On the basis of purely geometrical consideration, we found that the overall density of presumably homogeneous spheres $\rho(\text{PEO–PEOX/1})$ is ca. 0.3 g/mL, which is a summation of two contributions: $\rho(\text{PEO–PEOX}) = 0.15$ g/mL and $\rho(\text{Na}[1]) = 0.16$ g/mL. It means that even though the large nanoparticles, which formed at $\xi > 0.05$, are more compact than those observed for $\xi < 0.05$, they still resemble gel-like particles.

We also performed a few electrophoretic light scattering experiments. We measured zeta-potential of PEO–PEOX/1 nanospheres prepared in 0.1 M NaCl (ξ in the range 0.077–0.462) and diluted 10 times in order to decrease an ionic strength of the solution. Surprisingly, we observed (mostly) one narrow mode with negative zeta potential. Its value changed from -10 to -38 mV with increasing ξ . It suggests that the nanoparticles are stabilized by negative charge of PEOX/1 segments located within a surface region. It also explains the observation that the nanoparticles with low content of **1** are unstable: It is due to an insufficiently low value of zeta-potential of the PEO–PEOX/1 nanospheres.

NMR Study. We used ^1H NMR to estimate the fraction of polymer segments involved in the complex with different ξ and salt concentrations. The preparation of nanoparticle solutions and differences with respect to the LS titration mixing protocol are described in the Experimental Section. In Figure 3, we show ^1H NMR spectrum of pure PEO–PEOX and the PEO–PEOX/1 complex in 0.1 M NaCl with $\xi = 0.045$. It is evident that the peaks corresponding to hydrogen nuclei from PEOX (ethylene subunit 3.5 ppm; ethyl side group CH_2CH_3 2.4 ppm and CH_2CH_3 1.1 ppm) are broad in the spectrum of PEO–PEOX/1. It indicates a restricted mobility of the parts of PEOX chains, which are engaged in the complex formation. The PEO/1 segments are completely frozen, they do not contribute to the overall PEO signal, and it is not therefore broadened.^{6a,c} The ratios of integrated intensities of signals of ethylene subunits in PEO (round 3.7 ppm) and PEOX blocks (see Scheme 2) to those in a molecularly dissolved copolymer of the same concentration, which give the fractions of kinetically frozen monomer units, are shown in the insets of Figure 3 as a function of ξ (0.015 and 0.045). It is evident that the fraction of “frozen” PEOX backbones is appreciably higher (25% and 40%, for increasing ξ) than that of PEO units (5% and 20%, for

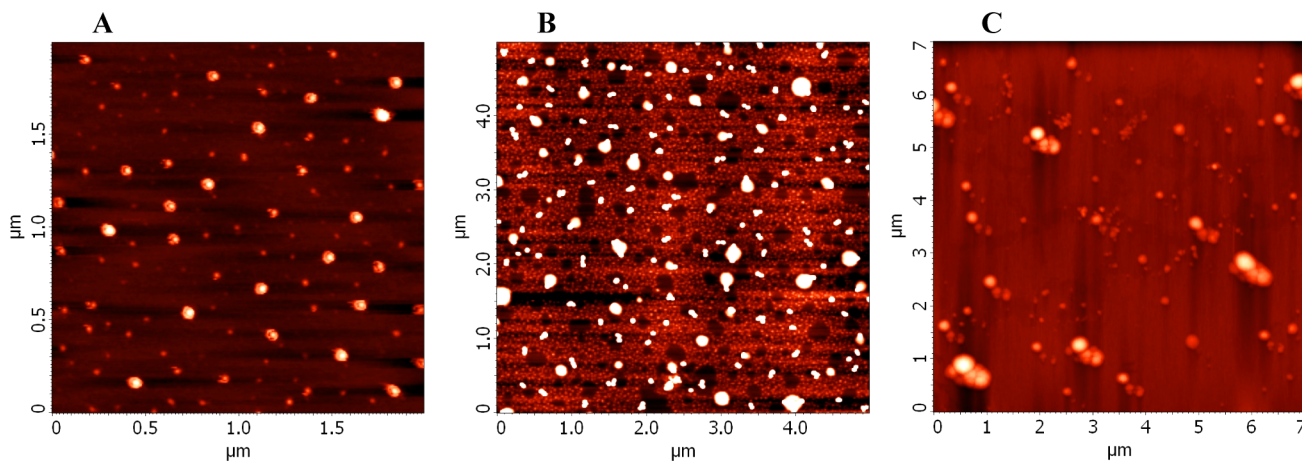


Figure 4. Typical AFM scans of PEO-PEOX/1 nanoparticles with (A) $\xi = 0.07$ in pure water, (B) $\xi = 0.07$ in 0.01 M NaCl, and (C) $\xi = 0.153$ in 0.1 M NaCl deposited on a flat mica surface.

increasing ξ). In both cases, it increases with ξ and almost does not depend on the presence of salt. The right inset in Figure 3 shows the fraction of kinetically frozen pending ethyl groups in the PEOX blocks (9% and 10%, for increasing ξ). We can see that their mobility does not depend on NaCl concentration, and it is much less affected by the content of **1**. It indicates that the mobility of the entire PEOX/1 segment is in fact higher than one would have expected from the immobilization of the ethylene subunits. It confirms our assumptions that metallacarborane interacts directly with the backbone of PEOX via dihydrogen bonds.

Assuming that both components are involved in the complex formation, we can calculate from the NMR results the following (details are given in Supporting Information): One copolymer chain consists of 114 PEO segments and 66 PEOX segments (see Scheme 2). One PEO₁₁₄-PEOX₆₆ chain interacts with ca. 3 molecules of Na[**1**] ($\xi = 0.015$) or ca. 8 molecules of Na[**1**] ($\xi = 0.045$). For $\xi = 0.015$, we obtained the following numbers of segments per polymer chain 6 frozen PEO segments and 17 frozen PEOX “backbones”, where only 6 from 17 PEOX segments involved in interaction with **1** are entirely frozen. For $\xi = 0.045$: 23 frozen PEO segments and 26 frozen PEOX “backbones”, where only 7 from 26 PEOX segments involved in interaction with **1** are entirely frozen. Assuming that only frozen segments are involved in the complex formation, there are 6–8 polymer segments involved in the complex formation per one metallacarborane molecule almost regardless of NaCl and **1** concentration. All the data suggest that there are still sufficiently large amounts of mobile segments that can stabilize the PEO-PEOX/1 nanospheres in solution with high ξ besides the negative zeta-potential: 73% of segments are not involved in the complex formation, and 83% of segments are mobile in the form of free PEO, PEOX, and PEOX/1 segments.

Further, we measured 2D ¹H NMR NOESY spectra to find out if the groups from POE and PEOX are close to each other, i.e., if PEO and PEOX blocks are intermixed and possibly interact with the same metallacarborane clusters. The NOESY spectrum is shown in Figure S3. A weak cross-correlation between ethylene signals from PEO and all the signals from PEOX is noticeable, but we have to keep in mind that the mobility of hydrogen atoms from PEO and PEOX groups, which form dihydrogen bonds to the same boron clusters, is restricted. Therefore, their contribution to the intensity of

pertinent diagonal peaks is very small, and the corresponding cross-correlation peaks are also very weak.

Microscopy Imaging. Valuable information on the shape and sizes of nanoparticles has been obtained by microscopy techniques (AFM and cryo-TEM). AFM images suggest (see Figures 4A–C) that at low ξ small compact particles exist in the solution. They merge together into irregular sponge-like structures and eventually into distinct spherical objects on the mica surface as salt and **1** concentrations increase. In Figure 5,

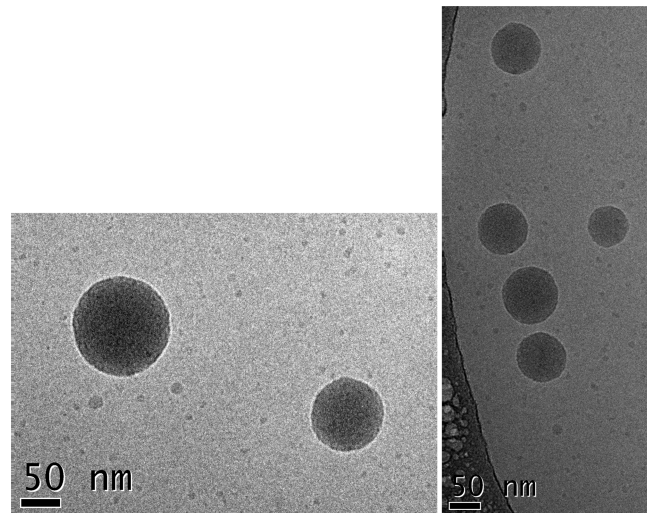


Figure 5. Typical cryo-TEM micrographs of PEO-PEOX/1 nanoparticles with $\xi = 0.153$ in 0.1 M NaCl.

there is the cryo-TEM image of PEO-PEOX/1 for $\xi = 0.153$ and 0.1 M NaCl. It unambiguously shows large homogeneous spherical objects, which coexist with small particles that have not been detected by DLS. The micrographs suggest that the nanospheres are homogeneous objects that do not exhibit core/shell structure (a corona has not been proven by cryo-TEM).

For the samples with $0.05 < \xi < 0.15$, we observe almost identical compact nanospheres (shown in Figure S4), but they have such a low contrast (low concentration of **1** within the nanospheres) that they are hardly seen as compared to the situation in Figure 5. It means that further addition of metallacarboranes does not change the shape and size of the already formed nanospheres. It indicates that there is a dynamic

equilibrium of metallacarborane between the nanospheres and bulk solution.

The cryo-TEM images together with LS and NMR data raise the question on the inner structure of the nanospheres. The block copolymers usually form the core/shell micelles when compatibilized with selective agents.^{10a–g} In the studied system, both blocks interact with **1** quite significantly. Because the presence of NaCl affects PEO and PEOX differently (PEO/**1** precipitates while PEOX/**1** does not), we assumed that its presence should differentiate the behavior of the blocks. However, the PEO–PEOX/**1** system does not behave according to our expectation—stable nanospheres, which do not have the core/shell structure, form in salted solutions.

On the basis of the above-described experimental data, we can propose the following explanation. Because it is known that PEO and PEOX chains are compatible¹¹ and Na[**1**] plays a role of an additional compatibilizer for both segments, nothing prevents the intermixing of PEO and PEOX blocks. Moreover, LS and other measurements indicate low density and hence high hydration, which implies a limited interaction of noncomplexed units from different blocks in the interior of PEO–PEOX/**1** nanoparticles. Therefore, a homogeneous intermixing of both blocks is highly probable. It means that one metallacarborane cluster can be involved in the complex with both PEO and PEOX segments at the same time. The nanospheres are stabilized in solution by PEO and PEOX segments not involved in the complex formation and by partly mobile PEOX/**1** segments bearing a negative charge.

Isothermal Calorimetry Titrations. To learn more about the thermodynamics of the coassembly process and to shed more light on the possible internal structure of aggregates, the interaction of PEO, PEOX, and PEO–PEOX with **1** was monitored by ITC (shown in Figures 6A–C). The studied processes are exothermic in all three cases. Pure homopolymer PEO (Figure 6A) shows a rather complicated behavior. The heats in pure water are relatively low in the ξ region up to 0.075, and then a shallow minimum appears close to ξ ca. 0.1. Thermodynamics of the complex formation in aqueous solution reflects the fact that the solution behavior of PEO in water is very complex.^{7b} It is also known to promote the structure of water.^{12a–d} Hence, a part of negative interaction heat is compensated by that of the disruption of the solvate shell after PEO units start to interact with metallacarborane clusters, and the interaction with water molecules is replaced by that with **1**.

The addition of NaCl (0.01 and 0.10 M) modifies the monitored ITC curves considerably. The observed thermal effects increase 2 times, and the shallow minimum becomes a deep one (Figure 6A). This minimum corresponds to the formation of a compact insoluble complex and indicates strong interaction between the components in the complex. The shift to lower ξ in 0.1 M NaCl as compared to 0.01 M NaCl reflects the fact that the complex precipitates earlier. The increase of the exothermic effect in salty solutions supports the assumption that dihydrogen bonding and changing water structure play a role. We observed similar effects in micellar systems with the PEO shell by means of solvent relaxation measurements.^{13a–c}

The curves for pure homopolymer PEOX look less complicated, but the behavior are not simple, either (Figure 6B). The titration curves do not acquire a typical sigmoidal shape of one site-binding model. The measured heat effects are significant. They are comparable with the deep minimum for PEO/**1**, even though the insoluble complex is not formed in this case. Although the interpretation of ITC data is usually

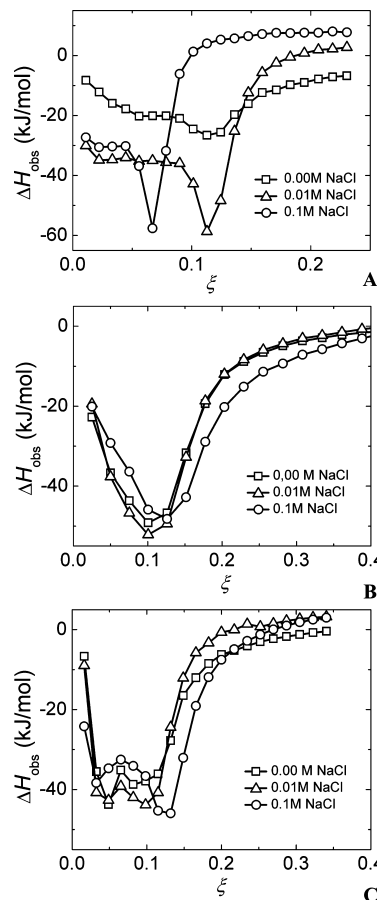


Figure 6. ITC thermograms for 0.0245 M Na[**1**] titrated into (A) 0.5 g/L PEO, (B) 0.5 g/L PEOX, and (C) 0.5 g/L PEO–PEOX, all in (squares) 0.00 M, (triangles) 0.01 M, and (circles) 0.10 M NaCl.

rather tricky, the shape suggests that there is a cooperation of interacting **1** molecules and PEOX segments.^{14a–d}

The curves describing the titration of PEO–PEOX are again very complex (Figure 6C). The exothermic peak is bimodal in the region $0.25 < \xi < 1.5$. The first minimum and a small decrease of measured exothermic values between both minima occur in the transition region between the first unstable region and the formation of more stable spherical particles with $R_H = 69$ nm. Even though the second minimum is attained in a similar ξ range as that for PEO, it is not related to a macroscopic precipitation of the sample. We can see a small shift with salt concentration, but no significant differences between ITC curves for PEO–PEOX in solutions with increasing NaCl content have been detected. This indicates further compatibilization of PEO and PEOX blocks by **1** and suggests some kind of cooperative effect in the case of PEO–PEOX. In other words, the thermochemistry of PEOX–PEO/**1** formation is not a simple sum of PEOX/**1** and PEO/**1** contributions. It supports the idea of binding of both blocks to one metallacarborane cluster and their mutual intermixing.

From the ITC curves shown in Figures 6A–C, we estimated the stoichiometry of the complex in 0.00, 0.01, and 0.10 M NaCl. We obtained the following numbers: PEO (6, 7, 12); PEOX (6, 6, 5); PEO–PEOX (7, 6, 6), respectively. It is close to number obtained by the NMR study. It is also clear from Figure 6C that the maximal loading capacity of the nanospheres in 0.1 M NaCl goes up to $\xi = 0.25$, which is equal to ca. 65% (w/w) of Na[**1**].

Small-Angle X-ray Scattering. To get even more insight into the internal structure of nanoparticles, we performed SAXS measurements on PEO–PEOX/1 in 0.1 M NaCl with constant polymer concentration (10 g/L) and increasing ξ . Three important facts have to be made clear before we start to discuss SAXS data: (i) The concentrations of PEO–PEOX for SAXS are 5 times higher than those used for SLS&DLS and other experimental techniques used (see Experimental Section). (ii) The available q -range is not sufficient for the study of large particles detected by means of SLS&DLS. We therefore used the SAXS measurements for investigation of the PEO–PEOX/1 internal structure only. (iii) The scattering contrasts, based on specific volumes (measured earlier for Na[1] and PEO),^{6a} for all three components are comparable (almost equal for PEO and 1 and slightly lower for PEOX).

The SAXS curves are shown in Figure 7. Scattering curve behavior at higher angles (q higher than 0.1 Å⁻¹) indicates the

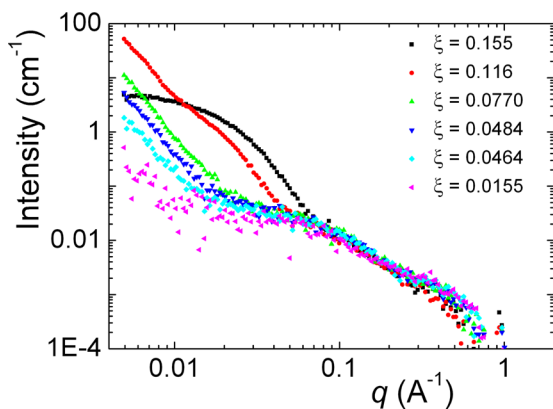


Figure 7. SAXS curves of 200 μ L 10 g/L PEO–PEOX in 0.1 M NaCl after addition of 20, 15, 10, 7.5, 6, and 2 μ L of 0.0245 M Na[1]. The corresponding values of ξ are also shown.

presence of highly swollen chains, which can coexist as free chains in the solution and as a part of internal structure of the large particles. The experimental points for all the samples are the same in this region, but the situation significantly changes for lower angles. It is possible only in the case, when the block copolymer PEO–PEOX remains swollen giving the stable scattering signal at higher angles. At low ξ values, metallacarborane can be randomly distributed within the large objects. Above the critical ξ value (≥ 0.116), Na[1] molecules can associate in small regions^{4d} inside the large swollen particles. Compact particles with sizes in the range of 10¹ nm in this ξ region were also confirmed by additional DLS measurements, and it is in agreement with the results from other methods. The scattering curve for the smallest ξ was fitted by Debye function in order to calculate molecular weight, M_w , of the swollen PEO–PEOX chains. The equation $M_w = (I_0/c)(N_a/\Delta b^2)$ gave value of $M_w = 9.5 \times 10^3$, where I_0 is the intensity, extrapolated to $q = 0$, N_a is Avogadro's number, and Δb^2 is the scattering contrast. It is close to M_w given by the manufacturer (11.5×10^3), which confirms our assumption stated above. The shape of the scattering curves with $\xi = 0.0464$ up to 0.116 indicates the presence of very large particles, the size of which is not possible to evaluate by SAXS.

However, the most important observation made by SAXS consists in the fact that there is no sign of correlation peaks in the region of high q between 0.1 and 1.0 Å⁻¹. It means that neither organized structures of metallacarborane clusters with

polymer coils nor collapsed domains have been proven in the studied system. It supports our assumption of intermixing of PEO&PEOX blocks and a gel-like nature of the nanospheres.

Concluding Remarks on the PEO–PEO/1 Self-Assembly. A complex behavior of PEO–PEOX/1 nanoparticles and the fact that the association proceeds differently than that in both PEO and PEOX systems suggest that there does not exist one decisive factor only, which controls the coassembly. The observed behavior is a result of the interplay of several contributions including hydration and changes in water structure. A cooperative effect of associating polymer segments from both blocks also plays a non-negligible role.

As the density of nanoparticles is low and does not differ much from that of PEO shells in core–shell micelles that we have been studying for quite a long time,^{15a–d} we can combine pieces of knowledge gained in studies of PEO brush-like shells and PEO/1 systems and try to explain the observed complex behavior. In studies of the core–shell systems with dense shells formed by long PEO blocks, contrary to our expectation we often observed that the systems were not stable enough. Our attempts to change the conditions (D₂O addition, changes in salt concentration, etc.) sometimes caused precipitation. From the literature, it is known that each PEO unit requires more than 3 water molecules for its full hydration and that the structure of water is promoted in the vicinity of the chain.^{12a–d} Our fluorescence studies (time-resolved anisotropy and solvent relaxation) indicated that the entropy decrease accompanying the increase of water structure in micellar shells may destabilize the system. Further, the presence of ions, which disrupt the water structure, affects the solvation and mobility of PEO and consequently also the stability of micellar solutions.

In the studied system, both blocks are water-soluble, but PEO and PEOX blocks differ in hydrophilicity.⁹ Further, both of them participate in the complex formation with Na[1]. Because the blocks are compatible and further compatibilized by interaction with metallacarborane compound, they intermix. Gel-like particles cross-linked by 1 are formed. The NMR study suggests that significant parts of both types of chains remain free. Both blocks are hydrated which is important from the point of view of solubility and stability of aggregates. However, PEO and PEOX segments compete for water molecules to reach the optimum hydration inside the particles.

Studies Aimed at the Preparation of Medicinally Relevant Systems. The last part of our study is targeted to the application of results and ideas described in the preceding paragraphs toward a drug delivery of boron cluster compounds. The question was whether PEO–PEOX would interact also with metallacarborane conjugates, inhibitors of HIV protease. We studied a series of the inhibitors 2–7 (structures shown in Scheme 1).^{4a–e} Almost all of them are sparingly soluble in water (7 is an only exception due to the presence of charged and highly soluble borane cluster attached to the span), and they form ill-defined aggregates in aqueous solutions, which is typical for almost all metallacarborane conjugates.^{4d} The solubility is even lower in salted solutions due to a common-ion effect (it drops at least 10 times for all the inhibitors except 7).^{4e} We therefore determined an increase of solubility of the inhibitors after the addition of 10 g/L PEOX–PEO in 0.154 M NaCl solution (physiological saline). The results are summarized in Table 1 together with hydrodynamic radii, R_h , of the corresponding aggregates and nanoparticles. It is clearly evident that PEO–PEOX interacts with all the inhibitors. It manifests itself in the substantial increase of solubility (ca. 10

Table 1. Solubility Increase and Changes in Hydrodynamic Radii, R_h , of Inhibitors after Addition of PEO–PEOX in 0.154 M NaCl

compd	absorbance increase at λ 300 nm	R_h/nm inhibitor	R_h/nm inhibitor + polymer
2	9 times	235	152
3	21 times	627	138
4	3 times	531	114
5	11 times	511	114
6	4 times	550	168
7		197	24

times on average) and formation of nanoparticles with lower dimensions as compared to the aggregates of pure inhibitors. The topology of the nanoparticles was briefly checked by AFM (not shown). In general, the nanoparticles are of round shape comparable to those of PEO–PEOX/1 nanospheres. Since the results are promising, we are planning biochemical experiments in cell cultures in order to explore an inhibition activity of the nanoparticles loaded by the inhibitors against HIV protease. The results will be published in a drug delivery oriented journal. However, some selected data have been included here to substantiate our research on the model system.

CONCLUSIONS

In order to prepare novel hybrid nanoparticles containing cobalt bis(1,2-dicarbollide) anion, **1**, with potential utilization, we studied hydrophilic and biocompatible poly(2-ethyloxazoline), PEOX, as a stabilizing block because poly(ethylene oxide), PEO, is not suitable for these purposes. As proven by our experimental study, the homopolymer PEOX interacts with Na[1] in aqueous media and forms the PEOX/1 complex, which, similarly to PEO/1, is stabilized by dihydrogen bonds between polymeric backbone and boron clusters (C–H···H–B). The PEOX/1 complex is water-soluble, while the PEO/1 composite precipitates in water. Hence, we focused our interest in the double hydrophilic block copolymer PEO–PEOX. We carried out a combined experimental study on PEO–PEOX/1 mixtures differing in metallacarborane content and NaCl concentration by standard scattering, microscopy, and spectroscopy techniques.

As concerns PEO–PEOX block copolymer, both blocks interact with metallacarborane, and PEO–PEOX/1 forms stable spherical nanoparticles in 0.1 M NaCl aqueous solution containing sufficiently high amount of **1**. Their inner structure surprisingly does not exhibit a distinct core/shell structure. Furthermore, neither PEO/1 nor PEOX/1 domains were detected within the nanoparticles. The multimethodical study shows that both blocks are intermixed and cross-linked by **1**. These gel-like nanospheres are stabilized by hydrated free parts of both blocks and mainly by soluble PEOX/1 segments bearing a negative charge (all together ca. 85% of polymeric segments are mobile). It means that much higher inhibitor loadings can be achieved in comparison with the case that the drug interacts with one block only. From ITC experiments, the loading capacity of PEO–PEOX/1 nanospheres in 0.1 M NaCl is up to 65% (w/w) of Na[1]. We observed that the preparation protocol does not affect the inner structure of the stable nanospheres. However, it affects the size of the prepared nanoparticles, and therefore it allows controlling it. The systems differing in length and number of both PEO and PEOX blocks as well as overall architecture of the polymer

chains are under investigation, and results will be presented in a separate communication.

We also demonstrated that the stable hybrid nanoparticles could be prepared also by mixing of PEO–PEOX with metallacarborane conjugates (inhibitors of HIV protease) in physiological saline. This observation is important for medical applications because (metalla)carborane-based inhibitors are usually sparingly soluble in physiological saline, and their incorporation in polymeric carriers increases substantially their “effective solubility”. However, we noticed in our preliminary biochemical experiments *in vitro* that inhibitors bind too strongly to PEO–PEOX. In other words, the polymeric nanoparticles “compete” with HIV protease for metallacarborane molecules, and their inhibition activity is therefore deteriorated to a certain extent. The challenge is to control a metallacarborane release from the hybrid nanospheres in cell cultures. Another point we would like to address in our forthcoming research is a role of counterions because we have dealt almost exclusively with sodium salts of metallacarboranes in our previous studies.

ASSOCIATED CONTENT

S Supporting Information

Further experimental SLS, DLS, NMR, and cryo-TEM data. This material is available free of charge via the Internet at <http://pubs.acs.org>.

AUTHOR INFORMATION

Corresponding Author

*Tel +420221951292; Fax +420224919752; e-mail pavel.matejicek@natur.cuni.cz (P.M.).

Notes

The authors declare no competing financial interest.

ACKNOWLEDGMENTS

The authors acknowledge financial support of the Grant Agency of the Academy of Sciences of the Czech Republic IAAX00320901, the Grant Agency of the Czech Republic P106/12/0143 and P208/12/P236, and long term Research Plans of the Ministry of Education of the Czech Republic MSM 0021620857. The authors thank Bohumír Grüner from IIC Prague for providing of metallacarborane samples and Jiří Zedník for assistance with NMR measurements.

REFERENCES

- (a) Scholz, M.; Hey-Hawkins, E. *Chem. Rev.* **2011**, *111*, 7035.
- (b) Lesniowski, Z. J. New Opportunities in Boron Chemistry for Medical Applications. In *Boron Science: New Technologies and Applications*; Hosmane, N. S., Ed.; CRC Press: New York, 2012; pp 3–19. (c) Bregadze, V. I.; Sivaev, I. B. Polyhedral Boron Compounds for BNCT. In *Boron Science: New Technologies and Applications*; Hosmane, N. S., Ed.; CRC Press: New York, 2012; pp 181–207.
- (d) Sibrian-Vazquez, M.; Vicente, M. G. H. Boron Tumor Delivery for BNCT: Recent Developments and Perspectives. In *Boron Science: New Technologies and Applications*; Hosmane, N. S., Ed.; CRC Press: New York, 2012; pp 209–241. (e) Vinas, C.; Nunez, R.; Teixidor, F. Large Molecules Containing Icosahedral Boron Clusters Designed for Potential Applications. In *Boron Science: New Technologies and Applications*; Hosmane, N. S., Ed.; CRC Press: New York, 2012; pp 701–740. (f) Hawthorne, M. F. *Angew. Chem., Int. Ed.* **1993**, *32*, 950.
- (g) Hawthorne, M. F. *Mol. Med. Today* **1998**, *4*, 174. (h) Hawthorne, M. F.; Lee, M. W. *J. Neuro-Oncol.* **2003**, *62*, 33. (i) Barth, R. F.; Soloway, A. H.; Goodman, J. H.; Gahbauer, R. A.; Gupta, N.; Blue, T. E.; Yang, W. L.; Tjarks, W. *Neurosurgery* **1999**, *44*, 433. (j) Tjarks, W. J.

- Organomet. Chem.* **2000**, *614*, 37. (k) Hawthorne, M. F.; Maderna, A. *Chem. Rev.* **1999**, *99*, 3421. (l) Soloway, A. H.; Tjarks, W.; Barnum, B. A.; Rong, F. G.; Barth, R. F.; Codogni, I. M.; Wilson, J. G. *Chem. Rev.* **1998**, *98*, 1515. (m) Lesnikowski, Z. *J. Collect. Czech. Chem. Commun.* **2007**, *72*, 1646. (n) Satapathy, R.; Dash, B. P.; Maguire, J. A.; Hosmane, N. S. *Collect. Czech. Chem. Commun.* **2010**, *75*, 995. (o) Bregadze, V. I.; Sivaev, I. B.; Glazun, S. A. *Anti-Cancer Agents Med. Chem.* **2006**, *6*, 75. (p) Crossley, E. L.; Ziolkowski, E. J.; Coderre, J. A.; Rendina, L. M. *Mini-Rev. Med. Chem.* **2007**, *7*, 303. (q) Tsuji, M.; Koiso, Y.; Takahashi, H.; Hashimoto, Y.; Endo, Y. *Biol. Pharm. Bull.* **2000**, *23*, 513. (r) Issa, F.; Kassiou, M.; Rendina, L. M. *Chem. Rev.* **2011**, *111*, 5701. (s) Grimes, R. N. In *Carboranes*; Academic Press: New York, 2011; pp 1053–1082.
- (2) (a) Plesek, J. *Chem. Rev.* **1992**, *92*, 269. (b) Llop, J.; Masalles, C.; Vinas, C.; Teixidor, F.; Sillanpaa, R.; Kivekas, R. *Dalton Trans.* **2003**, *4*, 556. (c) Masalles, C.; Llop, J.; Vinas, C.; Teixidor, F. *Adv. Mater.* **2002**, *14*, 826. (d) Gentil, S.; Crespo, E.; Rojo, I.; Friang, A.; Vinas, C.; Teixidor, F.; Gruner, B.; Gabel, D. *Polymer* **2005**, *46*, 12218. (e) Crespo, E.; Gentil, S.; Vinas, C.; Teixidor, F. *J. Phys. Chem. C* **2007**, *111*, 18381. (f) Masalles, C.; Borros, S.; Vinas, C.; Teixidor, F. *Adv. Mater.* **2000**, *12*, 1199. (g) Farras, P.; Juarez-Perez, E. J.; Lepsik, M.; Luque, R.; Nunez, R.; Teixidor, F. *Chem. Soc. Rev.* **2012**, *41*, 3445.
- (3) (a) Matejicek, P.; Cigler, P.; Prochazka, K.; Kral, V. *Langmuir* **2006**, *22*, 575. (b) Matejicek, P.; Cigler, P.; Olejniczak, A. B.; Andrysiak, A.; Wojtczak, B.; Prochazka, K.; Lesnikowski, Z. *J. Langmuir* **2008**, *24*, 2625. (c) Kubat, P.; Lang, K.; Cigler, P.; Kozisek, M.; Matejicek, P.; Janda, P.; Zelinger, Z.; Prochazka, K.; Kral, V. *J. Phys. Chem. B* **2007**, *111*, 4539. (d) Rak, J.; Jakubek, M.; Kaplanek, R.; Matejicek, P.; Kral, V. *Eur. J. Med. Chem.* **2011**, *46*, 1140. (e) Uchman, M.; Jurkiewicz, P.; Cigler, P.; Gruner, B.; Hof, M.; Prochazka, K.; Matejicek, P. *Langmuir* **2010**, *26*, 6268.
- (4) (a) Cigler, P.; Kozisek, M.; Rezacova, P.; Brynda, J.; Otwinowski, Z.; Pokorna, J.; Plesek, J.; Gruner, B.; Doleckova-Maresova, L.; Masa, M.; Sedlacek, J.; Bodem, J.; Krausslich, H. G.; Kral, V.; Konvalinka, J. *Proc. Natl. Acad. Sci. U. S. A.* **2005**, *102*, 15394. (b) Kozisek, M.; Cigler, P.; Lepsik, M.; Fanfrlik, J.; Rezacova, P.; Brynda, J.; Pokorna, J.; Plesek, J.; Gruner, B.; Grantz Saskova, K.; Vaclavikova, J.; Kral, V.; Konvalinka, J. *J. Med. Chem.* **2008**, *51*, 4839. (c) Rezacova, P.; Pokorna, J.; Brynda, J.; Kozisek, M.; Cigler, P.; Lepsik, M.; Fanfrlik, J.; Rezac, J.; Grantz Saskova, K.; Sieglova, I.; Plesek, J.; Sicha, V.; Gruner, M.; Oberwinkler, H.; Sedlacek, J.; Krausslich, H. G.; Hobza, P.; Kral, V.; Konvalinka, J. *J. Med. Chem.* **2009**, *52*, 7132. (d) Rezacova, P.; Cigler, P.; Matejicek, P.; Lepsik, M.; Pokorna, J.; Gruner, B.; Konvalinka, J. Medicinal Application of Carboranes: Inhibition of HIV Protease. In *Boron Science: New Technologies and Applications*; Hosmane, N. S., Ed.; CRC Press: New York, 2012; pp 41–70. (e) Rak, J.; Dejlova, B.; Lampova, H.; Kaplanek, R.; Matejicek, P.; Cigler, P.; Kral, V. *Mol. Pharmaceutics* **2013**, *10*, 1751.
- (5) (a) Harada, A.; Kataoka, K. *Prog. Polym. Sci.* **2006**, *31*, 949. (b) Zhao, Q.; Ni, P. H. *Prog. Chem.* **2006**, *18*, 768. (c) Rodriguez-Hernandez, J.; Checot, F.; Gnanou, Y.; Lecommandoux, S. *Prog. Polym. Sci.* **2005**, *30*, 691. (d) Gil, E. S.; Hudson, S. A. *Prog. Polym. Sci.* **2004**, *29*, 1173. (e) Lavasanifar, A.; Samuel, J.; Kwon, G. S. *Adv. Drug Delivery Rev.* **2002**, *54*, 169. (f) Matejicek, P.; Uchman, M.; Lepsik, M.; Srnec, M.; Zednik, J.; Kozlik, P.; Kalikova, K. *ChemPlusChem* **2013**, *78*, 528.
- (6) (a) Matejicek, P.; Zednik, J.; Uselova, K.; Plestil, J.; Fanfrlik, J.; Nykanen, A.; Ruokolainen, J.; Hobza, P.; Prochazka, K. *Macromolecules* **2009**, *42*, 4829. (b) Matejicek, P.; Brus, J.; Jigounov, A.; Plestil, J.; Uchman, M.; Prochazka, K.; Gradzielski, M. *Macromolecules* **2011**, *44*, 3847. (c) Uchman, M.; Cigler, P.; Gruner, B.; Prochazka, K.; Matejicek, P. *J. Colloid Interface Sci.* **2010**, *348*, 129.
- (7) (a) Luxenhofer, R.; Han, Y.; Schulz, A.; Tong, J.; He, Z.; Kabanov, A. V.; Jordan, R. *Macromol. Rapid Commun.* **2012**, *33*, 1613. (b) Sedlacek, O.; Monnery, B. D.; Filippov, S. K.; Hoogenboom, R.; Hruby, M. *Macromol. Rapid Commun.* **2012**, *33*, 1648.
- (8) Okur, H. I.; Kherb, J.; Cremer, P. S. *J. Am. Chem. Soc.* **2013**, *135*, 5062.
- (9) Casse, O.; Shkilnyy, A.; Linders, J.; Mayer, C.; Haussinger, D.; Volkel, A.; Thunemann, A. F.; Dimova, R.; Colfen, H.; Meier, W.; Schlaad, H.; Taubert, A. *Macromolecules* **2012**, *45*, 4772.
- (10) (a) Cohen Stuart, M. A.; Hofs, B.; Voets, I. K.; de Keizer, A. *Curr. Opin. Colloid Interface Sci.* **2005**, *10*, 30. (b) Bronich, T. K.; Keifer, P. A.; Shlyakhtenko, L. S.; Kabanov, A. V. *J. Am. Chem. Soc.* **2004**, *127*, 8236. (c) Uchman, M.; Stepanek, M.; Prevost, S.; Angelov, B.; Bednar, J.; Appavou, M. S.; Gradzielski, M.; Prochazka, K. *Macromolecules* **2012**, *45*, 6471–6480. (d) Uchman, M.; Prochazka, K.; Gatsouli, K.; Pispas, S.; Spirkova, M. *Colloid Polym. Sci.* **2011**, *289*, 1045. (e) Uchman, M.; Stepanek, M.; Prochazka, K.; Mountrichas, G.; Pispas, S.; Voets, I. K.; Walther, A. *Macromolecules* **2009**, *42*, 5605. (f) Matejicek, P.; Uchman, M.; Lokajova, J.; Stepanek, M.; Prochazka, K.; Spirkova, M. *J. Phys. Chem. B* **2007**, *111*, 8394. (g) Uchman, M.; Gradzielski, M.; Angelov, B.; Tosner, Z.; Oh, J.; Chang, T.; Stepanek, M.; Prochazka, K. *Macromolecules* **2013**, *46*, 2172.
- (11) Xu, S. Q.; Tang, T.; Huang, B. T.; Yin, C. M. *Acta Chim. Sin. (Engl. Ed.)* **1998**, *56*, 445.
- (12) (a) Kjellander, R.; Florin, E. J. *Chem. Soc., Faraday Trans. 1* **1981**, *77*, 2053. (b) Blanazs, A.; Warren, N. J.; Lewis, A. L.; Armes, S. P.; Ryan, A. J. *Soft Matter* **2011**, *7*, 6399. (c) Smart, T. P.; Mykhaylyk, O. O.; Ryan, A. J.; Battaglia, G. *Soft Matter* **2009**, *5*, 3607. (d) Ke, F.; Mo, X.; Yang, R.; Wang, Y.; Liang, D. *Macromolecules* **2009**, *42*, 5339.
- (13) (a) Humpolickova, J.; Stepanek, M.; Prochazka, K.; Hof, M. *J. Phys. Chem. A* **2005**, *109*, 10803. (b) Sachl, R.; Stepanek, M.; Prochazka, K.; Humpolickova, J.; Hof, M. *Langmuir* **2008**, *24*, 288. (c) Prochazka, K.; Matejicek, P.; Stepanek, M.; Limpouchova, Z.; Hof, M.; Humpolickova, J.; Sachl, R.; Schroeder, J. *Proc. SPIE—Int. Soc. Opt. Eng.* **2010**, *7571*, 757104.
- (14) (a) Olofsson, G.; Loh, W. *J. Braz. Chem. Soc.* **2009**, *20*, 577. (b) Lad, M. D.; Ledger, V. M.; Briggs, B.; Green, R. J.; Frazier, R. A. *Langmuir* **2003**, *19*, 5098. (c) Brown, A. *Int. J. Mol. Sci.* **2009**, *10*, 3457. (d) Freiburger, L. A.; Auclair, K.; Mittermaier, A. K. *ChemBioChem* **2009**, *10*, 2871.
- (15) (a) Stepanek, M.; Humpolickova, J.; Prochazka, K.; Hof, M.; Tuzar, Z.; Spirkova, M.; Wolff, T. *Collect. Czech. Chem. Commun.* **2003**, *68*, 2120. (b) Tsitsilianis, C.; Voulgaris, D.; Stepanek, M.; Podhajecka, K.; Prochazka, K.; Tuzar, Z.; Brown, W. *Langmuir* **2000**, *16*, 6868. (c) Stepanek, M.; Matejicek, P.; Humpolickova, J.; Prochazka, K. *Langmuir* **2005**, *21*, 10783. (d) Stepanek, M.; Uchman, M.; Prochazka, K. *Polymer* **2009**, *50*, 3638.